Aligned Single Wall Carbon Nanotube Polymer Composites Using an Electric Field

Cheol Park[1]*, John Wilkinson[2], Sumanth Banda[3], Zoubeida Ounaies[3], Kristopher E. Wise[1], Godfrey Sauti[4], Peter T. Lillehei[5], and Joycelyn S. Harrison[5]

[1]National Institute of Aerospace, MS-226, 6 West Taylor Street, Hampton VA, 23681

[2]Department of Electrical Engineering, Virginia Tech

[3]Department of Mechanical Engineering, Virginia Commonwealth University

[4]School of Physics, University of the Witwatersrand, Johannesburg, South Africa.

[5]Advanced Materials & Processing Branch, NASA Langley Research Center, Hampton VA, 23681, USA

*Corresponding author:

Cheol Park, Ph.D.

National Institute of Aerospace (NIA)

NASA Langley Research Center, MS-226

Hampton, VA 23681-2199 USA

Phone: 757-864-8360

Fax: 757-864-8312

E-mail: c.park@larc.nasa.gov

Abstract: While high shear alignment has been shown to improve the mechanical properties of SWNT-polymer composites, it is difficult to control and often results in degradation of the electrical and dielectric properties of the composite. Here, we report a novel method to actively align SWNTs in a polymer matrix, which allows for control over the degree of alignment of SWNTs without the side effects of shear alignment. In this process, SWNTs are aligned via field-induced dipolar interactions among the nanotubes under an AC electric field in a liquid matrix followed by immobilization by photopolymerization while maintaining the electric field. Alignment of SWNTs was controlled as a function of magnitude, frequency, and application time of the applied electric field. The degree of SWNT alignment was assessed using optical microscopy and polarized Raman spectroscopy and the morphology of the aligned nanocomposites was investigated by high resolution scanning electron microscopy. The structure of the field induced aligned SWNTs is intrinsically different from that of shear aligned SWNTs. In the present work, SWNTs are not only aligned along the field, but also migrate laterally to form thick, aligned SWNT percolative columns between the electrodes. The actively aligned SWNTs amplify the electrical and dielectric properties in addition to improving the mechanical properties of the composite. All of these properties of the aligned nanocomposites exhibited anisotropic characteristics, which were controllable by tuning the applied field conditions.

Keywords*:* Alignment; single wall carbon nanotube; nanocomposite; electric field; photopolymerization

INTRODUCTION

Single wall carbon nanotubes (SWNTs) have been considered for a number of applications because of their unique combinations of superb electrical, mechanical, and thermal properties.[1] Successful structural reinforcement of polymer matrices by SWNTs has been reported where significant improvement of mechanical properties was achieved at very low SWNT loadings.[2-7] Recently sensing and actuating capabilities of SWNTs and SWNT-polymer composites have been also studied in response to temperature, chemical vapors, strain, stress, electrochemical, and electrical stimuli.[8-13] However, integrating both structural and sensing/actuating functionalities in a single entity has rarely been achieved because of lack of control over SWNT dispersion and orientation in a given polymer matrix. Shear force is frequently used for aligning inclusions along the flow direction to reinforce mechanical properties. Although shear alignment of SWNTs can improve mechanical properties in the shear direction, electric and dielectric properties tend to decrease along the shear direction as well as the perpendicular direction with increasing SWNT orientation. Kumar et al.[6] showed that a well-aligned 10wt% SWNT-PBO (poly(*p*-phenylene benzbisoxazole)) composite fiber possessed significant mechanical reinforcement while exhibiting electrically insulating behavior along the fiber direction. This loading level is at least three orders of magnitude higher than the percolation concentration of an unaligned SWNT polymer composite. This conductivity behavior can be understood by considering the lower statistical probability of contact among the aligned fibers along the orientation direction and is consistent with the predictions of excluded volume theory.[14,15] These results indicate that shear alignment of SWNTs may not be a practical method of augmenting nanocomposite properties beyond mechanical

reinforcement. The only way of circumventing this difficulty with shear processing would be to further increase the loading of SWNTs, which would limit its versatility for developing multifunctional materials for specific demands.

In the present report, a novel method is introduced which allows for control over the physical properties of a SWNT-polymer composite by alignment under an AC electric field. Alignment of SWNTs by electric and magnetic fields has previously been reported,[16-20] though usually in dilute solutions during solvent evaporation or filtration. More recently, very limited alignment of SWNTs in a polymer matrix was achieved using a magnetic field[21] and thermally cured aligned SWNT epoxy composites under an electric field was reported.[22] In this letter, control over the degree of alignment of SWNTs in a photopolymerizable monomer solution was achieved by investigating the influence of the applied field strength, frequency, and application time. The conductivity and dielectric properties can be tailored several orders of magnitude by adjusting these parameters.

EXPERIMENTAL

The photopolymerizable monomer used in this study is a blend of urethane dimethacrylate (UDMA) and 1,6-hexanediol dimethacrylate (HDDMA) at the ratio of 9 to 1. The viscosities were 12.5 Pa·s and 7.0 x 10^{-3} Pa·s for UDMA and HDDMA, respectively. Both UDMA and HDDMA monomers can be polymerized by blue light with camphorquinone as a photoinitiator and N,N-dimethylaminoethyl methacrylate as an accelerator. The monomers could be solidified to a depth of 3 mm within about 3 s under illumination by intense blue light. Single wall carbon nanotubes (SWNTs) synthesized by a high pressure CO (HiPco) method (CNI, Texas) were used as multifunctional

inclusions. A schematic of the alignment and photopolymerization apparatus is shown in Figure 1. Either a pure UDMA/HDDMA(9/1) (UH) monomer solution or 0.03wt%SWNT/UH composite solution was added in the 1mm deep cell between the electrodes spaced at 2.3mm. The 0.03wt% was selected as a sub-percolation threshold base on the percolation study of various SWNT-polymer composites, where the lowest percolation threshold was found around 0.05wt%. This concentration also allows to cure the control sample through the 1mm deep effectively. An AC power supply (Trek model 50/750) and a function generator (Hewlett Packard 33120A) were used to control the applied electric field conditions. The influence of the AC field parameters were studied by varying the field strength (10 to 250V_{p-p} as a step function), time (1 to 60 min), and frequency (10^{-3} to 10^{5}Hz). The photopolymerizable solution was polymerized using blue light with a hand-held light gun (Optilux 501) for 1 min while the field was being applied. The solidified samples were cured by blue light another 10 min and then annealed at 110˚C in an oven overnight to further complete polymerization. The cured samples were first investigated with an optical microscope. The samples were then sectioned and polished for electrical and dielectric measurements, and fractured for high resolution scanning electron microscopy (HRSEM) study. The AC conductivity and dielectric constants of the SWNT/UH composites were measured with a Novocontrol Broadband Dielectric Converter and a Solatron SI1260 Impedance/Gain-Phase Analyzer. Polarized Raman scattering spectra were collected using a Thermo Nicolet Almega™ dispersive visible Raman spectrometer. A 785 nm incident laser light excitation was used with a polarizer and the laser beam was focused on the sample using an optical microscope. Low excitation laser power (10%) was used to minimize sample heating.

RESULTS AND DISCUSSION

Within the present experimental setup, there are three controllable parameters for influencing the degree of SWNT alignment: electric field strength, application time, and the frequency of the applied AC field. Optimal values for these parameters have been obtained by varying each in turn, while holding the other two constant. This actually requires an iterative process in which the values held fixed are determined by a number of preliminary experiments. In what follows, only the final set of experiments is described.

For the electric field strength optimization, the field application time was held fixed at 10 min while two AC frequencies were investigated, 100 Hz and 10 kHz. Various selected electric fields were applied as a step function at this condition. These conditions were judiciously selected to probe the electric field effect independently based on preliminary experiments. It was found that the degree of alignment was strongly dependent on the applied electric field and the same trends were observed with the two AC frequencies studied, 100 Hz and 10kHz. No alignment was observed below $65V_{p-p}$ with noticeable alignment beginning to appear at $75V_{p-p}$ (37.5V/2.3mm = 16.3kV/m for a step function). The degree of alignment continued to increase up to a plateau value at $200V_{p-p}$ (43.5kV/m). Increasing the voltage beyond this point tended to induce more skewed alignment near the electrodes possibly due to excessive thermal energy. Beyond $300V_{p-p}$, the temperature of the composite increased significantly due to Joule heating (higher than 100˚C), which tended to locally disrupt or bend the aligned nanotubes. Next, the effect of field application time was studied at a fixed voltage of $200V_{p-p}$ and

frequency of 10kHz. These experiments showed that alignment began almost immediately and grew with increasing field application time until saturation was observed at around 10 min. Finally the effect of field frequency was studied at $200V_{p-p}$ for an application time of 10min. In this case the degree of alignment grew with increasing frequency, saturating at 10 Hz. Interestingly the SWNTs were observed to align at frequencies as low as 0.001 Hz to some degree, which is effectively a DC condition, albeit requiring a much longer field application time.

Optical microscopy was used for initial, qualitative evaluation of the degree of alignment. Figure 2(a) shows an optical micrograph of a SWNT/UH composite cured without an electric field, which reveals a relatively uniform dispersion overall with a few micrometer scale agglomerates and no preferential alignment or elongated features. Figure 2(b) shows a micrograph of the aligned composite prepared under $200V_{p-p}$, 10Hz, and 10min, where aligned SWNT bundles are seen along the field direction and the micrometer scale agglomerates were also aligned with their elongated axes along the field direction.

More detailed microstructures of the aligned SWNTs were investigated with high resolution scanning electron microscopy (HRSEM). The composites were microtomed either parallel or perpendicular to the field direction and examined without a conductive coating at a low voltage (below 1kV). Figure 3(a) shows the microtomed surface of the unaligned sample and the nanotubes could not be imaged due to the non-conducting behavior of the sample. In contrast, the microtomed surface of the aligned composites showed the ability to set up a stable electric field permitting visualization of the SWNTs that are part of the percolation network. Figure 3(b) shows the SWNT aligned along the

field, with some of the aligned clusters extending several hundred micrometers in length. The aligned clusters along the field are seen to be composed of a series of small SWNT clusters ranging from tens of nanometers to a few micrometers. Some of the aligned SWNT clusters lie parallel to one another and are connected with jagged or fray aligned clusters (coarsening). This aligned microstructure is reminiscent of the dielectrophoretic alignment and subsequent lateral coarsening of inclusions often observed in electrorheological or magnetorheological fluids.[23,24] This coarsening, which arises from the lateral migration among the aligned nanotubes, creates conductive percolation paths even at loadings as low as 0.03%. While alignment of SWNT bundles and clusters is evidently seen at higher magnification in Figure 3(c), alignment of individual SWNTs in the clusters was not discernible due to the severe bleaching near the clusters. (Note that the small upward spikes shown in the aligned SWNTs in Figure 3(c) were originated from the microtoming.) It is also notable that there was little indication of any electrophoretic effect that would be indicated by migration of SWNTs to the electrodes. Figure 3(d) shows a microtomed surface perpendicular to the electric field of the same aligned SWNT/UH composite. In this sample evenly distributed, round SWNT clusters were observed, which are believed to be the cross-sections of the aligned SWNT clusters shown in Figure 3(b). This indicates the distinct anisotropic nature of the aligned SWNT/UH composites and is similar to the anisotropic morphology observed in different composite systems with spherical or equiaxed inclusions obtained under electric fields.[23]

The degree of alignment of SWNTs in the aligned composite was also assessed by polarized Raman spectroscopy. This characterization relies on the fact that the Raman intensity of the tangential mode of SWNTs is sensitive to the polarizer angle. The

tangential mode intensity reaches a maximum when the polarized light is parallel to the nanotube axis[25] and decreases gradually as the angle of the polarizer increases from 0° (parallel to the nanotube axis) to 90° (perpendicular to the nanotube axis). The intensity begins to increase again as the angle of the polarizer increases from 90° to 180°. The tangential peaks (1591cm^{-1}) of the polarized Raman spectra for the aligned composite (10Hz) are shown at different angles in Figure 4. As expected, the maximum intensity was observed when the polarized light was parallel to the applied electric field direction (0˚) and the smallest intensity appeared when the polarized light was perpendicular to the field direction (90°). Similar results were obtained for the aligned composites with the frequency ranging from 10Hz to 100kHz. Note that the relative Raman intensity at 0° was similar to that at 180°. The polarized Raman results effectively demonstrate the preferential alignment of the individual SWNTs in the aligned SWNT bundles and clusters that resulted from the AC electric field.

Electrical Conductivity of SWNT/UH composites

The conductivities of the pristine matrix resin UH, and the unaligned and aligned composites, both at 0.03wt% SWNT, are shown in Figure 5 as a function of the measurement frequency. The Figure 5 shows the conductivities measured along the field direction, for composites aligned at several applied voltages. The conductivity of the pristine resin was 1.4 x 10^{-13} S/cm and that of the unaligned composite was 3.3 x 10^{-13} S/cm at 1Hz, revealing less than an order of magnitude increase in conductivity with incorporation of 0.03wt% SWNT. The conductivities of both of these samples increased linearly with the frequency on a logarithmic scale across most of the frequency range, indicating insulative behavior and therefore a lack of percolation at the 0.03wt% SWNT

loading. For the aligned composites, the conductivity of the samples parallel to the field did not noticeably increase until $50V_{p-p}$ and then increased significantly at $100V_{p-p}$ from 1.4×10^{-12} to 3.0×10^{-9} S/cm. Further increases were observed for higher alignment fields up to saturation at around $150V_{p-p}$, where the conductivity is on the order of 10^{-7} S/cm. Metallic behavior was observed for the samples aligned above $100V_{p-p}$, as indicated by the relatively constant conductivity observed at low frequencies (below 10^2Hz) with slight increase at higher frequencies (above 10^2Hz). These results indicate that the conductivity of the composites can be controlled over six orders of magnitude by controlling the strength of the aligning electric field.

The influence of the frequency of the applied electric field on the conductivity is shown in Figure 6. All of the aligned samples in the Figure 6 were formed under a field of $200V_{p-p}$ for 10min, at the various frequencies. The conductivity of the composite aligned at 0.01Hz AC, measured parallel to the field, was slightly higher than that of the unaligned composite but still showed insulating behavior. A significant increase was observed at 1Hz, with the conductivity increasing from 3.3×10^{-13} (No field) to 4.6×10^{-9} S/cm and moving into the metallic regime. At 10Hz the conductivity increases to 1.4×10^{-7} S/cm and reaches a plateau value of 10^{-6} S/cm at 100 Hz, saturating at higher frequencies. These results may indicate that, at very low frequencies, the misaligning forces such as Brownian motion and electrophoretic force are stronger than the aligning dielectrophoretic force, preventing or disrupting nanotube alignment. Above 1Hz, while electrophoresis becomes insignificant and the aligning dielectrophoretic force becomes more significant and increases to saturation above 100Hz. Similarly to the previous case of field strength, these results show that the conductivity of SWNT/UH composites can

be readily controlled by the AC frequency. Conductivities ranging from insulating (10^{-13} S/cm) to conductive (10^{-6} S/cm) can be achieved with a 0.03wt% SWNT loading, which is lower than the percolation concentration for an isotropic dispersion.[5,26,27] Although slight alignment was observed at lower frequencies (0.01 and 0.1Hz), it was not reflected in the conductivity of the composite, suggesting that the aligned clusters of the SWNT bundles percolate above 0.1Hz under these conditions.

The observation of increasing conductivity with increasing alignment of SWNTs is unexpected based on the excluded volume percolation theory of cylindrical inclusions in an insulating matrix.[14,15] In general, the concentration of conducting cylinders required to reach percolation is expected to increase with increasing degree of alignment, as shown in Figure 7. In the present composite, it is likely that the conductive path among the SWNTs bundles lies not only along the field direction, but also among the aligned clusters by lateral contacts. Remarkably, the conductivity of the composite perpendicular to the electric field alignment direction also increased with alignment by about two orders of magnitude, as shown in Figure 8. While the aligned clusters continued to grow by the accretion of small SWNT bundles or other aligned clusters longitudinally, the aligned clusters also attracted one another laterally. This lateral joining of aligned clusters resulted in the formation of crosslinks between aligned clusters with jagged or frayed ends, as shown in Figures 3(b) and (c) (coarsening). Figure 3(c) shows that some dots (cross-sections of the aligned SWNTs) were connected with neighbors to form short chains. This early stage of coarsening is responsible for the relatively high conductivity of the composite in the direction perpendicular to the aligning field. This proposed sequence of formation of the aligned structure under an AC field was previously reported

and described by a simple model.[23] In this picture, the electric field causes the SWNT bundles to first attract one another primarily along the field direction to form aligned SWNT bundle clusters, followed by lateral attractions that lead to crosslinking. Recall also the even distribution and nominally equivalent intercluster distances observed in Figure 3(c), which is consistent with previous observations.[23]

Dielectric Properties of SWNT/UH composites

The dielectric constants of the pristine UH, unaligned and aligned SWNT/UH composites (parallel to the alignment field) are shown as a function of frequency in Figure 9. All samples were aligned at 100Hz for 10 min with the various applied field strengths. The dielectric constant of the pristine UH and unaligned composite at 1 Hz were 5.2 and 25.2 at 0.03wt%SWNT, respectively. For samples prepared under higher aligning fields, the dielectric constant increased in the same way as the conductivity. No significant increases were observed up to $50V_{p-p}$, followed by more significant increases up to $100V_{p-p}$, where the dielectric constant reaches values over 600 at 1Hz. These increases continue up to a maximum value of around 1500 at $150V_{p-p}$, at which point saturation is observed. The composites prepared below $50V_{p-p}$ exhibit an insulating material behavior, while those prepared above that show conductive behavior, which is consistent with the conductivity results.

The electric field frequency also strongly influenced the dielectric behavior of the composites, as shown in Figure 10. The composite aligned at 0.01Hz exhibited little increase in dielectric constant over the unaligned composite, indicating lack of orientation at this frequency. For 1Hz aligned samples, however, the dielectric constant increased up to 900 and exhibited strong dispersion at a measurement frequency of 100Hz, suggesting

the presence of a perocolative path of aligned nanotubes along the field direction. The dielectric constant saturated at a value of over 1000 for samples aligned at frequencies above 100Hz. All of these results are completely consistent with the conductivity measurements. These experiments illustrate that the dielectric constant of the composites can be easily adjusted over three orders of magnitude by controlling the frequency and strength of the AC aligning field.

Having now established the alignment behavior of SWNTs in the UH matrix, it is of interest to attempt to understand these results within the context of a simple model which may enable the design of improved systems. Alignment in this system arises from the field-induced polarization of the nanotubes and the attraction and repulsion between the induced dipole moments.[28] The dipolar interaction competes with the thermal randomization (i.e. Brownian motion). Thus, alignment generally can only occur when the alignment force arising from dipolar interaction dominates.[28] For a spherical inclusion, the parameter defining the relative strengths of the dipolar interaction and thermal agitation is[29]

$$\lambda = \frac{\pi \varepsilon_0 \varepsilon_1 a^3 (\beta E)^2}{k_B T} \qquad (1)$$

where ε_0 is the permittivity of free space (8.854 x 10^{-12} F/m), ε_1 is the relative dielectric constant of the liquid resin (about 4.9 at 20Hz), a is the radius of the inclusion, E is the applied electric field, k_B is Boltzmann's constant (1.38 x 10^{-23}JK^{-1}), and T is the absolute temperature. When polarization arises from the mismatch of polarizability between the

matrix and inclusion, β is given by $(\varepsilon_2 - \varepsilon_1)/(\varepsilon_2 + 2\varepsilon_1)$, where ε_2 is the relative dielectric constant of the inclusion. But when the conductivity of the inclusion or matrix dominates, β is given by $(\kappa_2 - \kappa_1)/(\kappa_2 + 2\kappa_1)$, where κ_1 and κ_2 are the conductivity of the matrix and inclusion, respectively. For the present system, since the inclusion is a cylindrical nanotube, the effective radius of the inclusion a may be replaced by the radius of gyration (R_g) of the nanotube. The length of the nanotube (L) was around 3μm based on AFM study[30] and the radius of the nanotube (R) is about 0.5nm. Assuming the nanotube is a rigid cylinder, the radius of gyration of the nanotube is given by,[31]

$$a = R_g = ((R^2/2) + (L^2/12))^{1/2} \approx (L^2/12)^{1/2} \approx 0.87\mu\text{m}$$

The measured dielectric constant of a 2wt% SWNT-polyimide composite was approximately 100000 at 20Hz.[13] Therefore, we can reasonably assume that the inclusion dipole coefficient (β) approaches 1. On the other hand, a DC conductivity of approximately 10^2 S/cm was obtained from fitting the conductivity of SWNT/Polymer composties, using a two exponent phenomenological percolation equation.[26] This value, which is obtained from the conductivity of SWNT/polymer composites measured as a function of SWNT volume fraction, is comparable to those measured for SWNT mats (bucky papers).[32] The cured matrix is a capacitive insulating material, which has the conductivity of around 10^{-14} S/cm at 1Hz and the liquid oligomer was more conductive, but it has the conductivity still below 20 x 10^{-8} S/cm.[23] Therefore, the value β for DC or low frequency also approaches one. Therefore, either case, the value β is proper to be assumed as one.

To achieve alignment, the parameter λ, which is the ratio of polarization energy to thermal energy, must be greater than one. For the present system, the critical effective nanotube size for alignment, assuming that polarization arises from the polarizibility of the fluid and nanotubes, can be calculated from Eq. (1) for the field strengths used for the alignment. The dielectric constant of the liquid is 4.9 and the temperature reached a maximum of 40˚C under the applied field (43.5kV/m). If we assume that the dipole coefficient β is 1, the critical effective nanotube diameter is 0.67 μm at 43.5kV/m ($200V_{p-p}$) and 1.53 μm at 16.3kV/m ($75V_{p-p}$). Since the radius of gyration of nanotube was about 0.87 μm for 3 μm long nanotube, alignment is likely to occur under the present field conditions. This conclusion is even more sound in light of the fact that the SWNT bundles are much longer than single tubes. This alignment can be accelerated with time once the aligned clusters grow, since the effective diameter of nanotubes keeps growing.

CONCLUSION

The results presented above show that the conductivity and dielectric properties of aligned SWNT/UH composites can be tuned over a broad range by proper control of the applied field strength, frequency, and time. The structure of the aligned composites was visually investigated using HRSEM, which showed clear distinctions from composites prepared by passive alignment using shear processing. The unique crosslinked structure produced by the field alignment technique is expected to provide unique properties of the composite compared to the aligned structures created by high shear (spinning, extrusion, and so on). These aligned SWNT polymer composites enable control over electrical and dielectric properties in addition to mechanical reinforcement, which will enable the

development of multifunctional structural composites. The key feature of this approach is the novel ability to produce composites with the required properties for a specific application by simply tuning the applied field strength, frequency, and time.

ACKNOWLEDGEMENTS

Park and Wise appreciate the NASA University Research, Engineering and Technology Institute on Bio Inspired Materials (BIMat) under award no. **NCC-1-02037** for support in part.

REFERENCES AND NOTES

1. Saito, R.; Dresselhaus, G.; Dresselhaus, M. S. Physical Properties of Carbon Nanotubes, Imperial College Press, London, 1998.
2. Haggenmueller, R.; Gommans, H.; Rinzler, A.; Fischer, J.; Winey, K. Chem Phys Lett 2000, 330, 219.
3. Gong, X.; Liu, J.; Baskaran, S.; Voise, R. D.; Young, J. S. Chem Mater 2000, 12, 1049.
4. Qian, D.; Dickey, E.; Andrews R.; Rantell, T. Appl Phys Lett 2000, 76, 2868.
5. Park, C.; Ounaies, Z.; Watson, K.; Crooks, R.; Connell, J.; Lowther, S. E.; Siochi, E. J.; Harrison, J. S.; St. Clair, T. L. Chem Phys Lett 2002, 364, 303.
6. Kumar, S.; Dang, T. D.; Arnold, F. E.; Bhattacharyya, A. R.; Min, B. G.; Zhang, X.; Vaia, R. A.; Park, C.; Adams, W. W.; Hauge, R. H.; Smalley, R. E.; Ramesh, S.; Willis, P. A. Macromolecues 2002, 35, 9039.
7. Siochi, E. J.; Working, D. C.; Park, C.; Lillehei, P. T.; Rouse, J.; Topping, C. C.; Bhattacharyya, A. R.; Kumar, S. Composites B 2004, 35, 439.
8. Baughman, R. H.; Cui, C.; Zakhidov, A. A.; Iqbal, Z.; Barisci, J. N.; Spinks, G. M.; Wallace, G. G.; Mazzoldi, A.; De Rossi, D.; Rinzler, A. G.; Jaschinski, O.; Roth, S.; Kertesz, M. Science 1999, 284, 1340.
9. Wood, J. R.; Wagner, H. D. Appl Phys Lett 2000, 76, 2883.
10. Kim P.; Lieber, C. M. Science 1999, 286, 2148.
11. Kong, J.; Franklin, N. R.; Zhou, C.; Chapline, M. G.; Peng, S.; Cho, K.; Dai, H. Science 2000, 287, 622.
12. Sumanasekera, G.; Adu, C.; Fang, S.; Eklund, P. Phys Rev Lett 2000, 85, 1096.

13. Ounaies, Z.; Barnes, C.; Park, C.; Harrison J. S.; Lillehei, P. T. Submitted for publication.
14. Balberg, I.; Binenbaum, N.; Wagner, N. Phys Rev Lett 1984, 52, 1465.
15. Balberg, I.; Binenbaum, N.; Alexander, S.; Wagner, N. Phys Rev B 1984, 30, 3933.
16. Yamamoto, K.; Akita, S.; Nakayama, Y. Jpn J Appl Phys 1996, 35, L917.
17. Yamamoto, K.; Akita, S.; Nakayama, Y. J Phys D: Appl Phys.1998, 31, L34.
18. Chen, X. Q.; Saito, T.; Yamada, H.; Matsushige, K. Appl Phys Lett 2001, 78, 3714.
19. Nagahara, L. A.; Amlani, I.; Lewenstein, J.; Tsui, R. K. Appl Phys Lett 2002, 80, 3826.
20. Krupke, R.; Hennrich, F.; Löhneysen, H. v.; Kappes, M. M. Science 2003, 301, 344.
21. Kimural, T.; Ago, H.; Tobita, M.; Ohshima, S.; Kyotani, M.; Yumura, M. Adv Mater 2002, 14, 1380.
22. Martina, C. A.; Sandler, J. K. W.; Windle, A. H.; Schwarz, M. -K.; Bauhofer, W.; Schulte, K.; Shaffer, M. S. P. Polymer 2005, 46, 877.
23. Park C.; Roberston, R. E. Mater Sci Eng A 1998, 257, 295.
24. Tang, X.; Zhang, X.; Tao, R.; Rong, Y. J Appl Phys 2000, 87, 2634.
25. Rao, A. M.; Jorio, A.; Pimenta, M. A.; Dantas, M. S. S.; Saito, R.; Dresselhaus, G.; Dresselhaus, M. S. Phys Rev Lett 2000, 84, 1820.
26. McLachlan, D. S.; Chiteme, C.; Park, C.; Wise, K. E.; Lowther, S. E.; Lillehei, P. T.; Siochi E. J.; Harrison, J. S. J Poly Sci: Poly Phys, 2005, 43, 3273.
27. Z. Ounaies, C. Park, K. E. Wise, E. J. Siochi, and J. S. Harrison, Comp Sci Tech 2003, 63, 1637.

28. Pohl, H. A. Dielectrophoresis: the behavior of neutral matter in nonuniform electric fields, Cambridge: Cambridge University Press, 1978.

29. Gast, A. P.; Zukoski, C. F. Adv Coll Int Sci 1989, 30, 153.

30. Park, C.; Crooks, R. E.; Siochi, J.; Harrison, J. S.; Kenik, E.; Evans, N. Nanotechnology, 2003. 14, L11.

31. Rubinstein, M.; Colby, R. H. Polymer Physics, Oxford Univ Press, New York, p64, 2003.

32. Sreekumar, T. V.; Liu, T.; Kumar, S.; Ericson, L. M.; Hauge, R. H.; Smalley, R. E. Chem Mater 2003, 15, 175.

Figure legends

Figure 1. (a) Experimental set-up of photopolymerization of SWNT/UH composite under an electric field, (b) top-view of the alignment cell (aligned SWNTs shown as discontinuous lines).

Figure 2. Optical micrographs of (a) SWNT/UH composite cured without electric field, (b) SWNT-UH composite cured with electric field ($200V_{p-p}$, 10Hz, 10min). Note that the alignment of SWNTs along the applied electric field (EF ↕).

Figure 3. High resolution scanning electron micrographs (HRSEM) of unaligned (a) and aligned SWNT/UH composites ($200V_{p-p}$, 10Hz, 10min) microtomed surface parallel (b), (c) and perpendicular (d) to the electric field. Aligned nanotubes appeared as dark features.

Figure 4. Polarized Raman spectra showing Tangential peak of SWNTs aligned by AC electric field $200V_{p-p}$, 10Hz, 10min.

Figure 5. Conductivities of UH and SWNT/UH composites prepared at various electric fields (100Hz, 10min).

Figure 6. Conductivities of UH and SWNT/UH composites prepared at various frequencies ($200V_{p-p,}$ 10min).

Figure 7. Percolation volume fraction as a function of orientation of SWNT with different nanotube diamters. ($\langle \sin(\gamma) \rangle = 0$ for perfect orientation, =1 for random).

Figure 8. Conductivities of UH and SWNT/UH composites measured parallel and perpendicular to the field used in sample preparation.

Figure 9. Dielectric constants of UH and SWNT/UH composites prepared at various electric fields.

Figure 10. Dielectric spectra of pristine UH and SWNT/UH composites prepared at different frequencies.

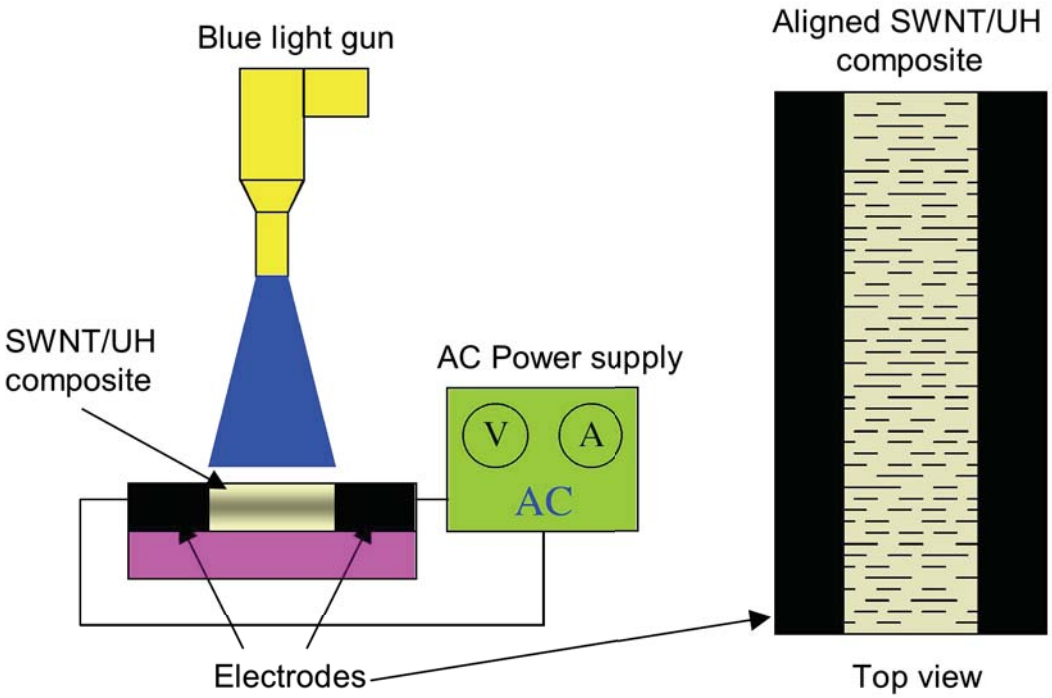

Figure 1.

Park, Wilkinson, Banda, Ounaies, Wise, Sauti, Lillehei, Harrison

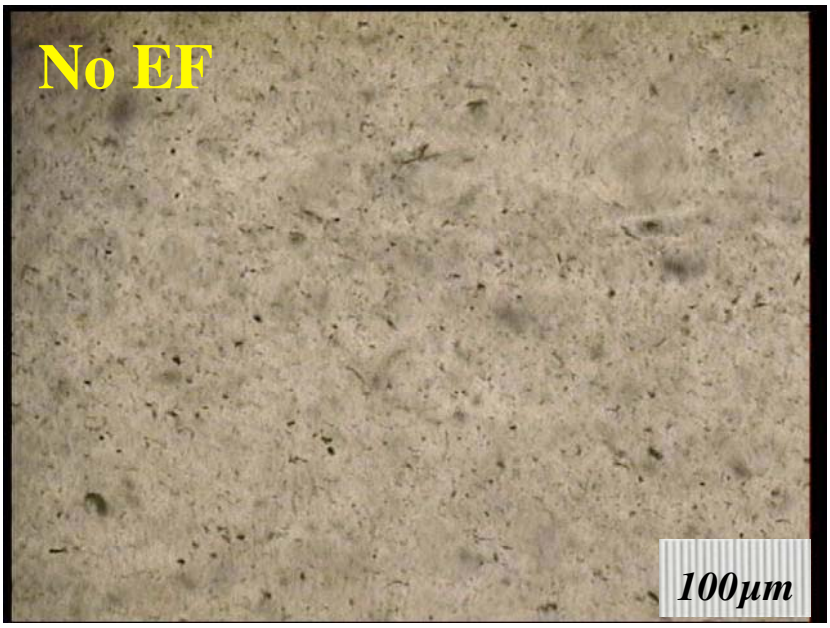

(a)

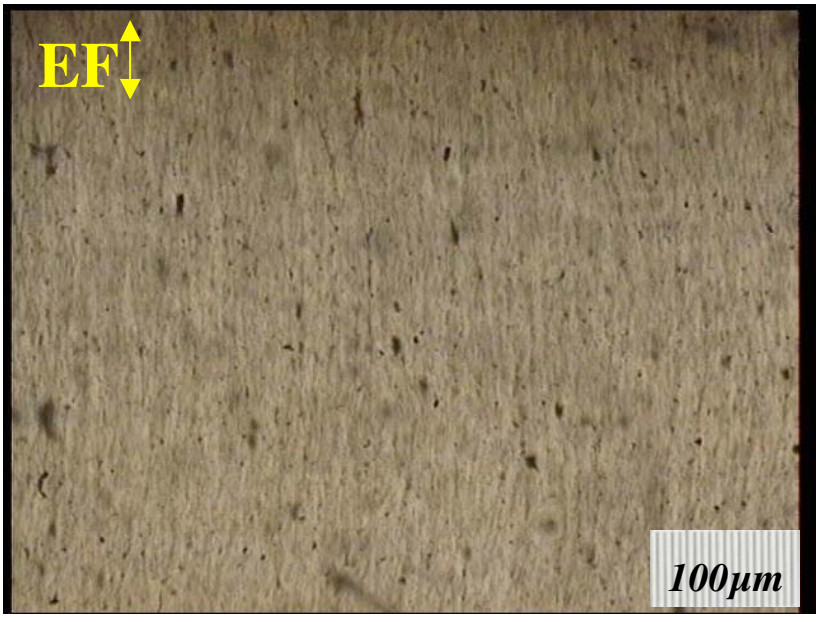

(b)

Figure 2.

Park, Wilkinson, Banda, Ounaies, Wise, Sauti, Lillehei, Harrison

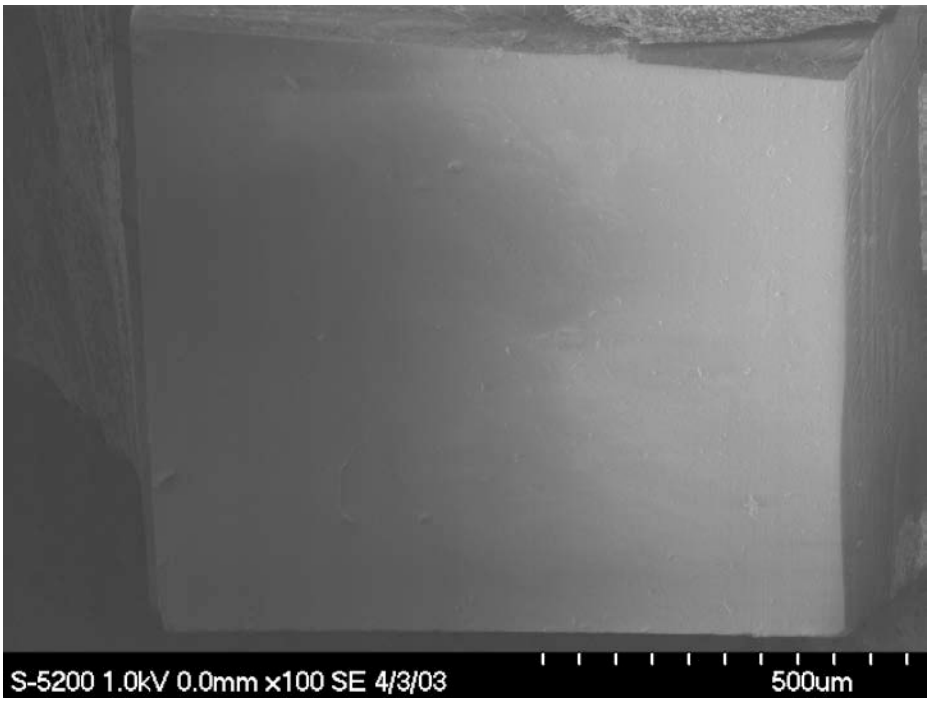
S-5200 1.0kV 0.0mm x100 SE 4/3/03
500um

(a)

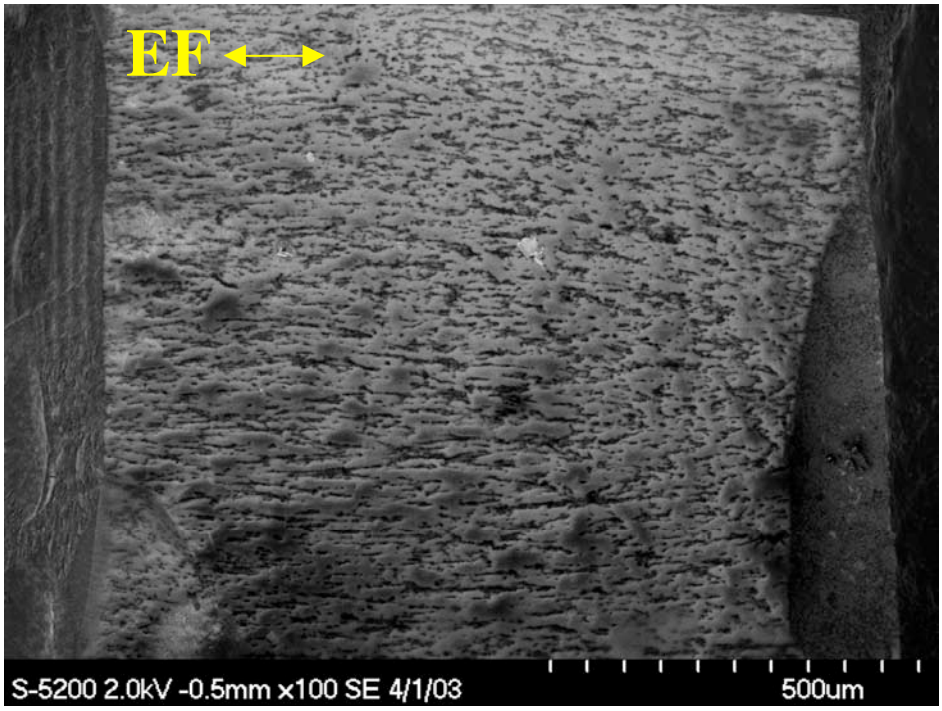
EF
S-5200 2.0kV -0.5mm x100 SE 4/1/03
500um

(b)

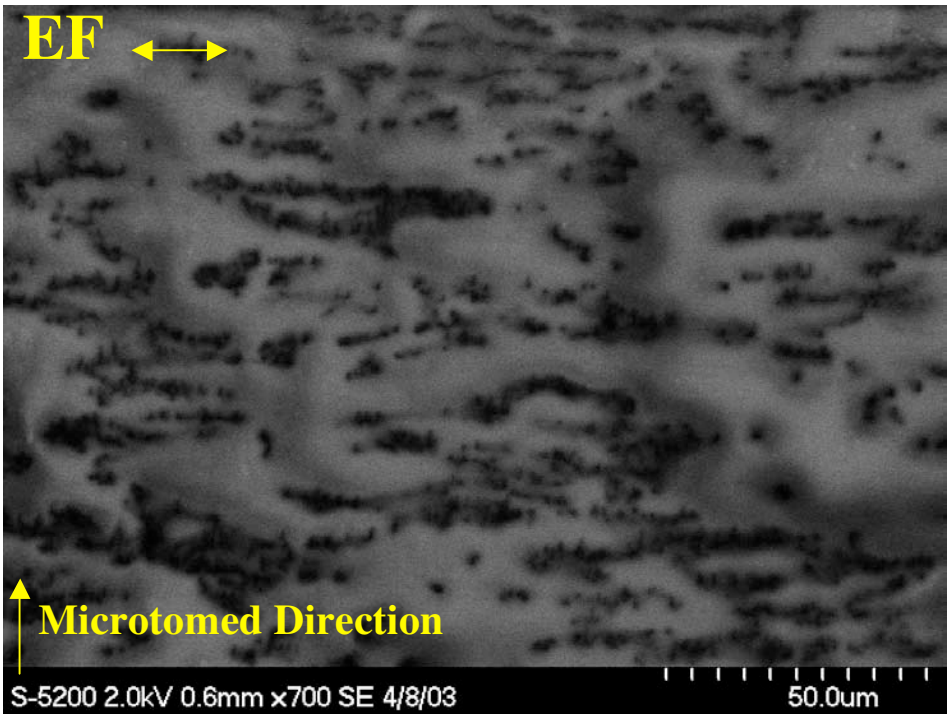

(c)

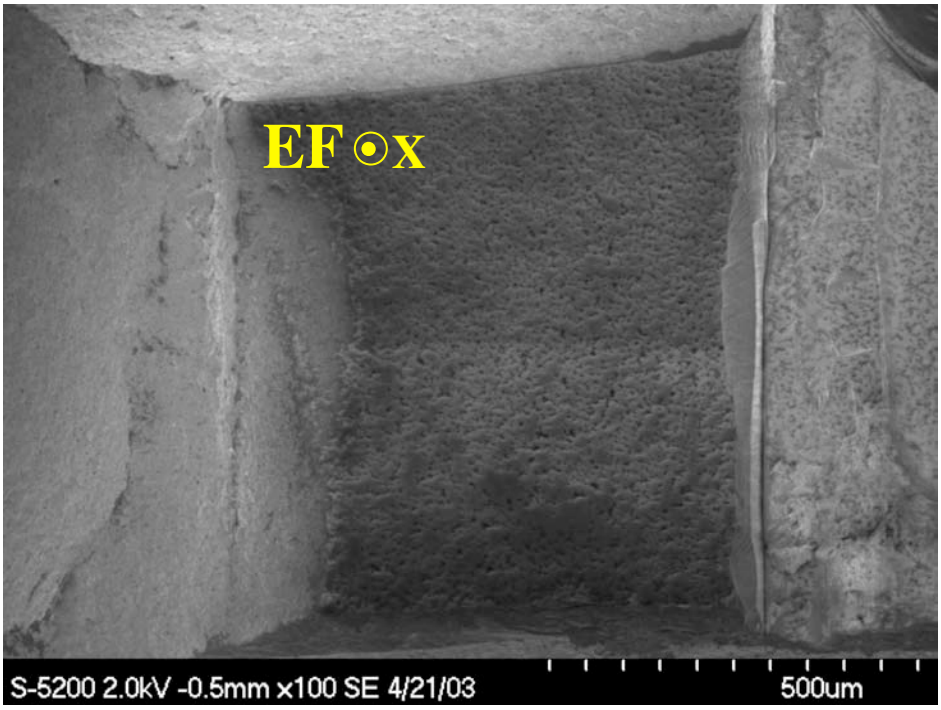

(d)

Figure 3.

Park, Wilkinson, Banda, Ounaies, Wise, Sauti, Lillehei, Harrison

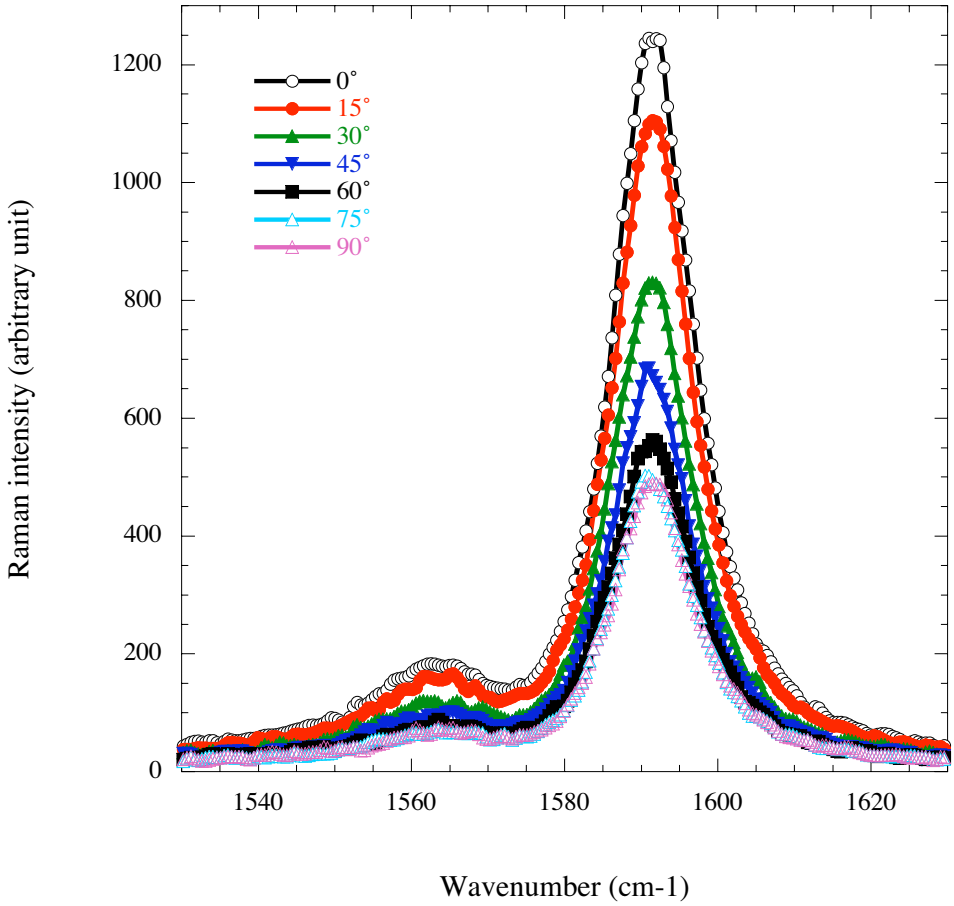

Figure 4.

Park, Wilkinson, Banda, Ounaies, Wise, Sauti, Lillehei, Harrison

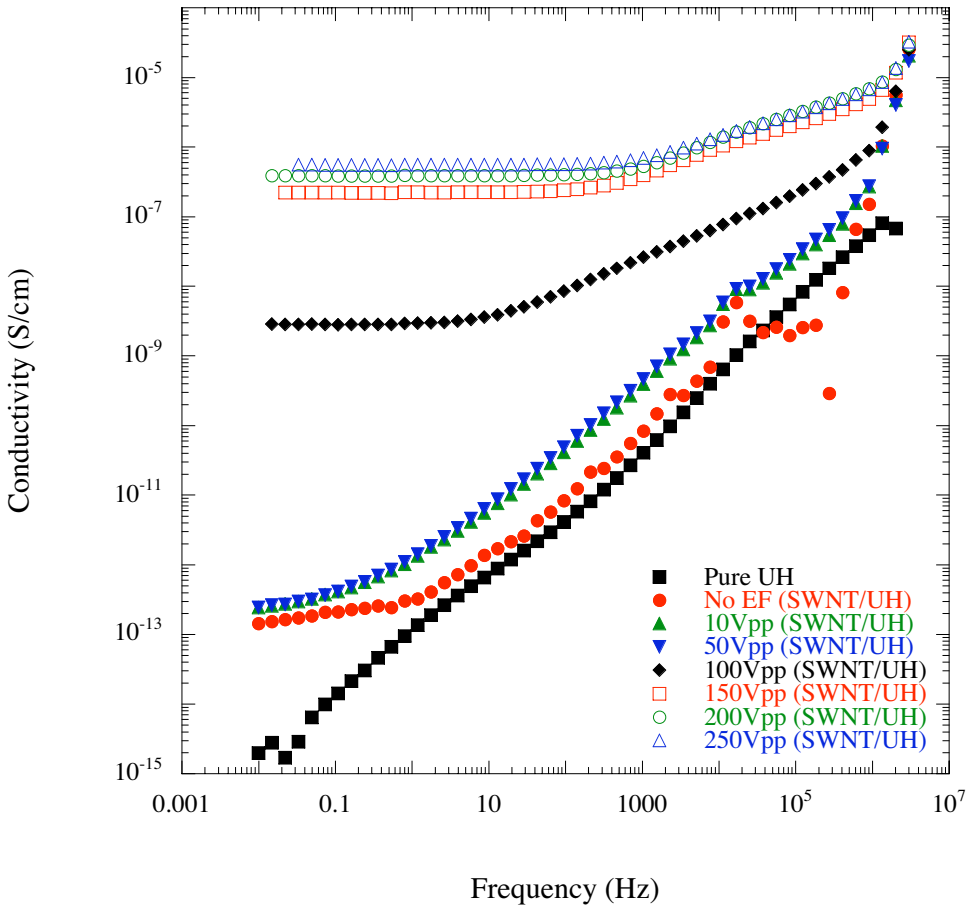

Figure 5.

Park, Wilkinson, Banda, Ounaies, Wise, Sauti, Lillehei, Harrison

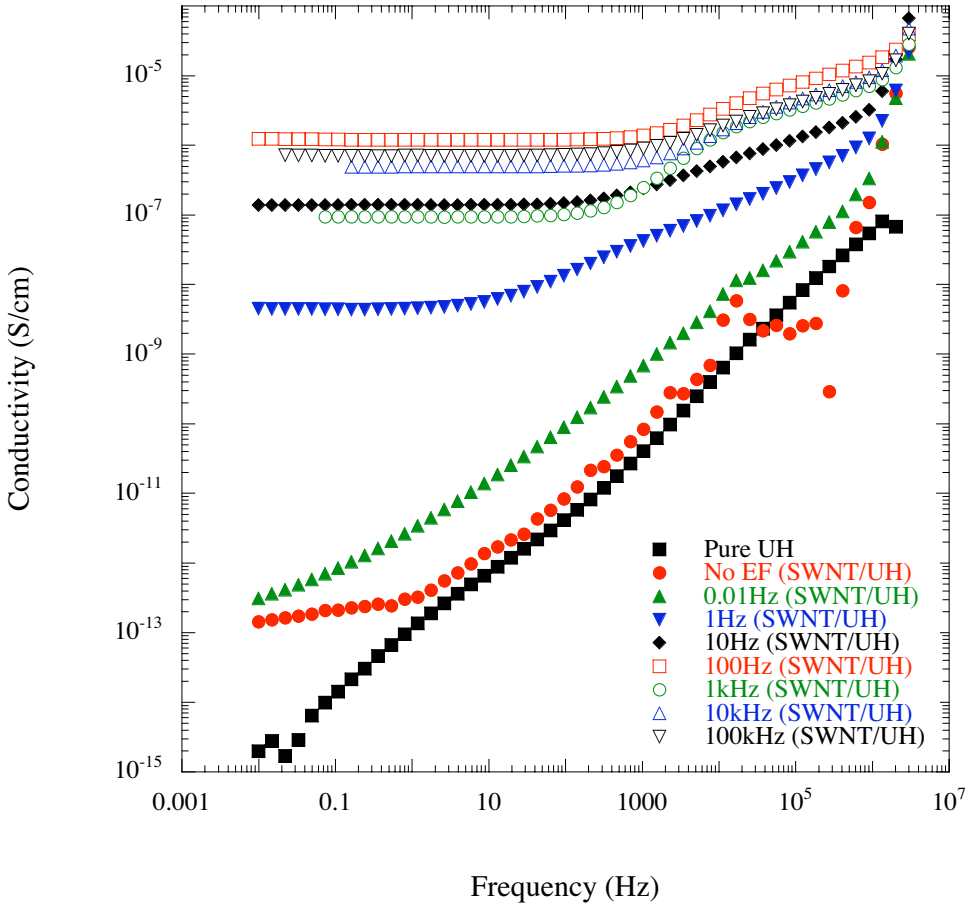

Figure 6.

Park, Wilkinson, Banda, Ounaies, Wise, Sauti, Lillehei, Harrison

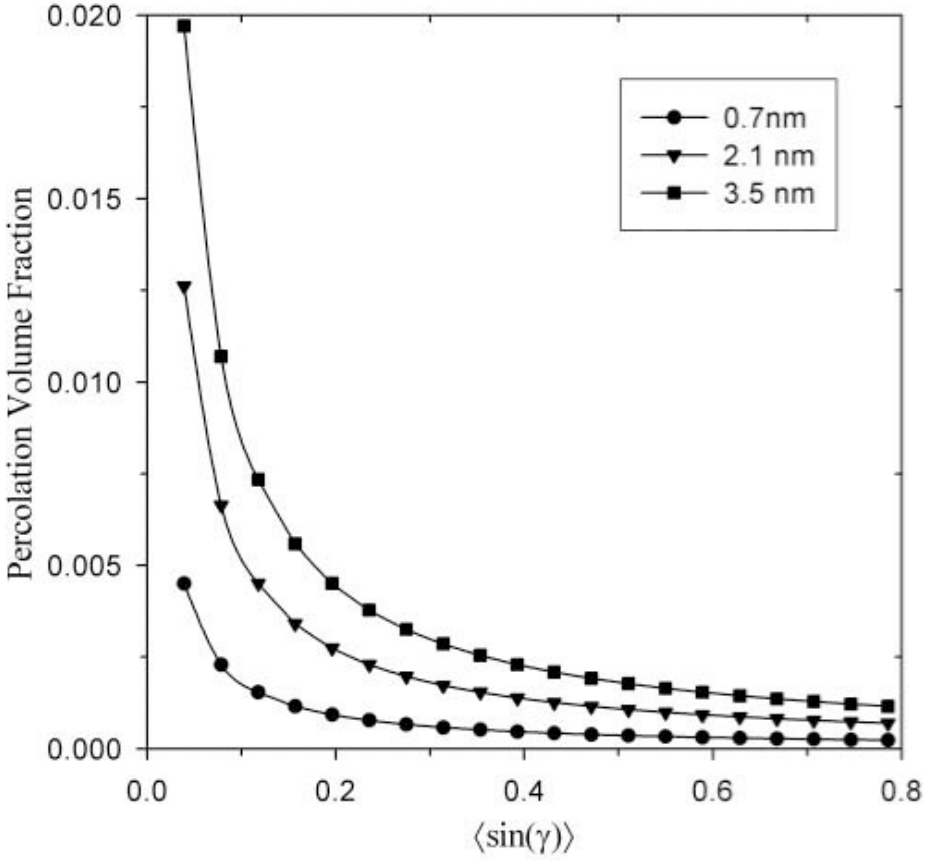

Figure 7.

Park, Wilkinson, Banda, Ounaies, Wise, Sauti, Lillehei, Harrison

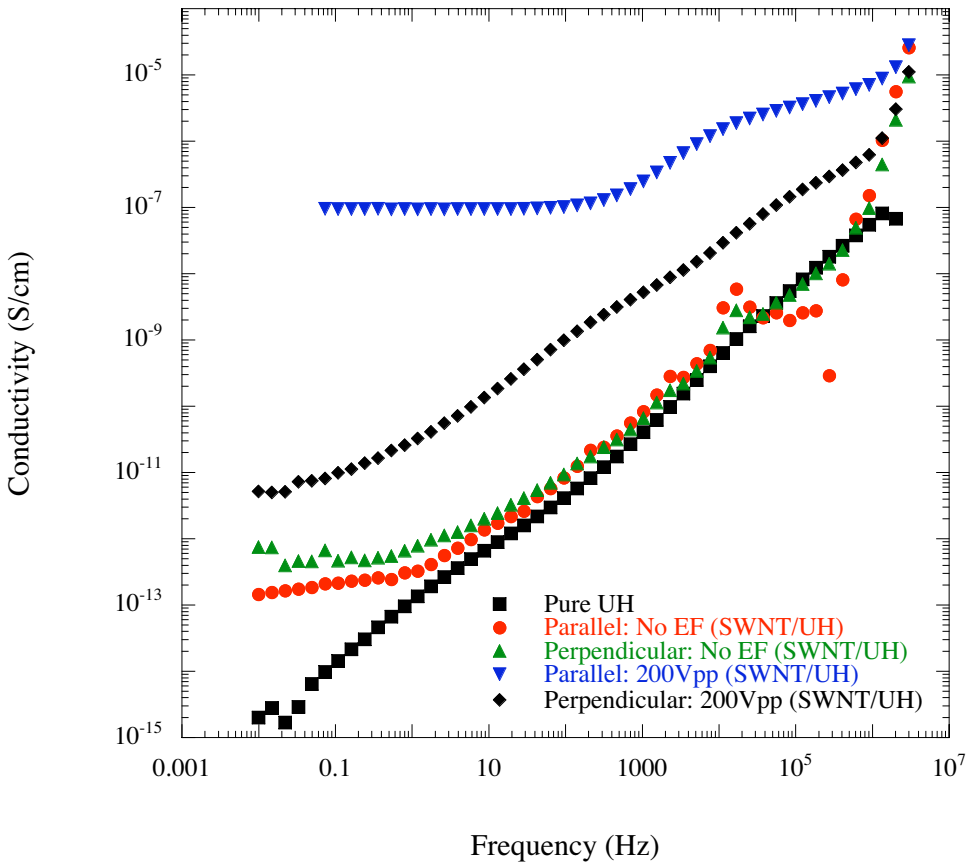

Fgiure 8.

Park, Wilkinson, Banda, Ounaies, Wise, Sauti, Lillehei, Harrison

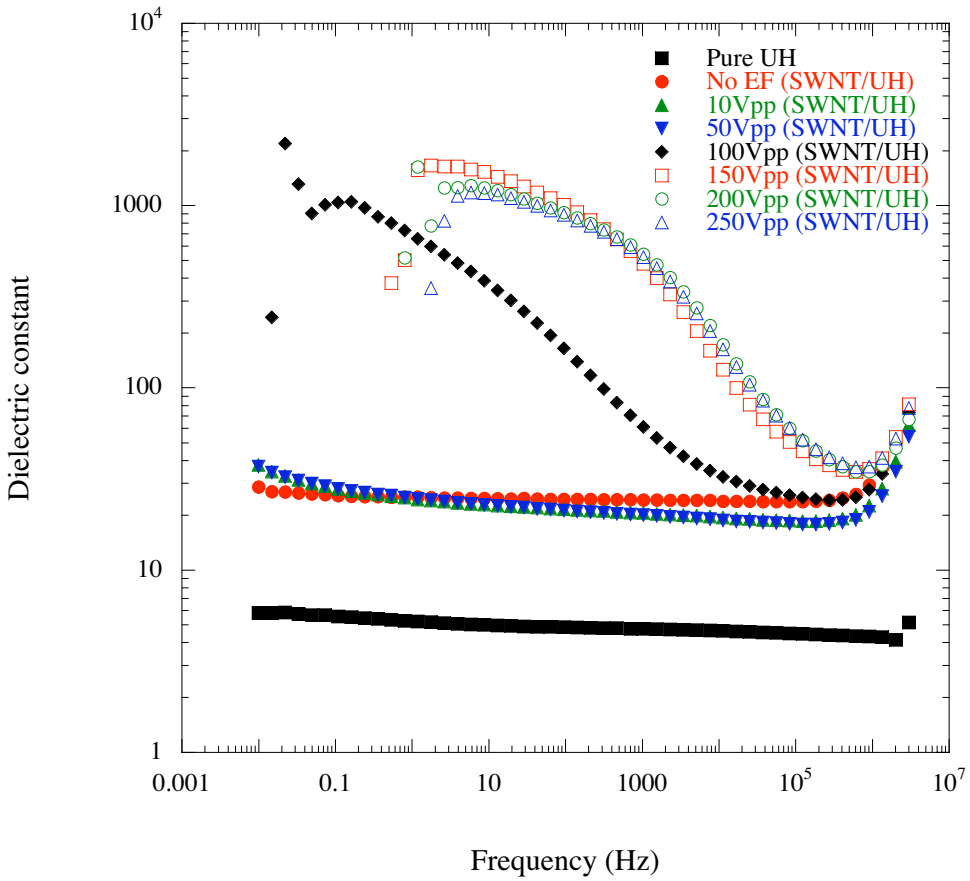

Figure 9.

Park, Wilkinson, Banda, Ounaies, Wise, Sauti, Lillehei, Harrison

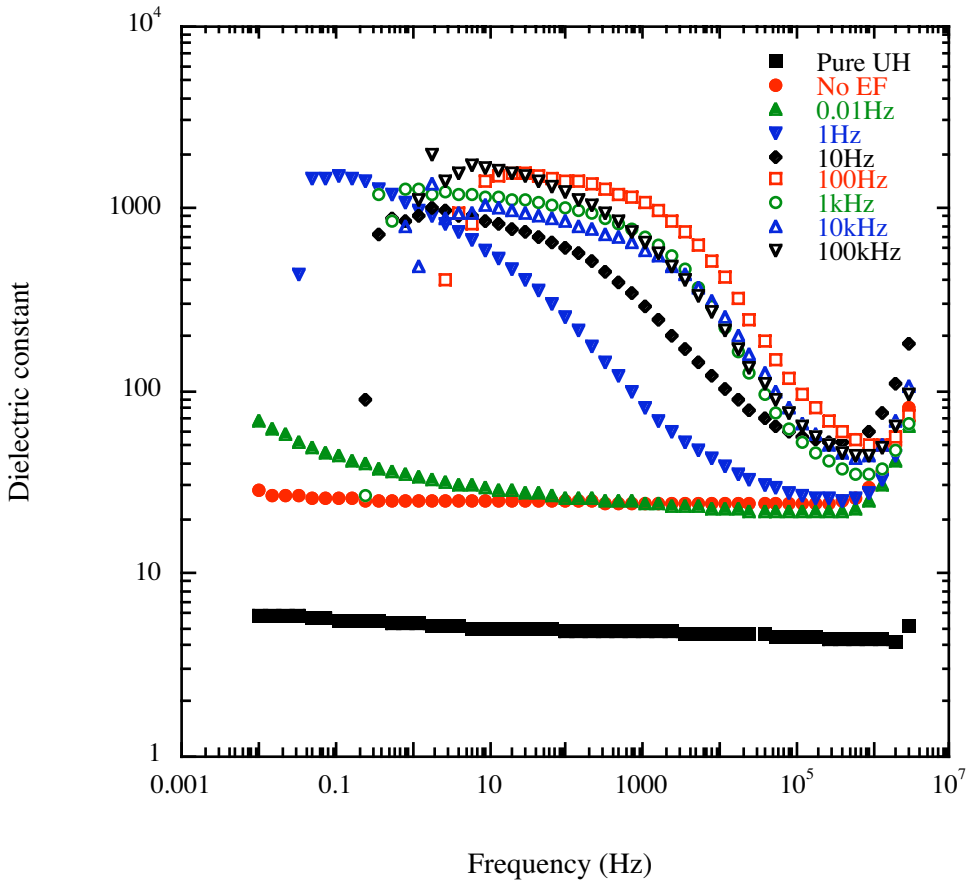

Figure 10.

Park, Wilkinson, Banda, Ounaies, Wise, Sauti, Lillehei, Harrison